

ELASTIC SCATTERING SPECTROSCOPY AS A DIAGNOSTIC TOOL FOR DIFFERENTIATING PATHOLOGIES IN THE GASTROINTESTINAL TRACT: PRELIMINARY TESTING

Judith R. Mourant,[†] Irving J. Bigio,[†] James Boyer,[†] Tamara M. Johnson,[†] JoAnne Lacey,[†]
Anthony G. Bohorfoush,[‡] and Mark Mellow^{*}

[†]Los Alamos National Laboratory, CST-4, MS-E535, Los Alamos, New Mexico 87545; [‡]Medical College of Wisconsin, Department of Gastroenterology, 9200 W. Wisconsin Ave., Milwaukee, Wisconsin 53226; and ^{*} University of Oklahoma Medical School, 3366 NW Expressway, Suite 400, Oklahoma City, Oklahoma 73112

(Paper JBO-039 received Sep. 11, 1995; revised manuscript received Dec. 26, 1995; accepted for publication Dec. 26, 1995)

ABSTRACT

We report preliminary clinical testing of elastic-scattering spectroscopy for the detection of pathologies of the gastrointestinal tract. Tissue pathologies are detected and diagnosed using spectral measurements of elastically scattered light in an optical geometry that results in sensitivity to both the absorption and scattering properties of the tissue, over a wide range of wavelengths (300 to 750 nm). The system employs a small fiber optic probe, which is amenable to use with most endoscopes or catheters, or to direct surface examination, as well as interstitial needles. In this paper we report the results of preliminary clinical measurements on various organ sites of the gastrointestinal tract. In several instances the data indicate promise for this diagnostic method to distinguish malignant and dysplastic conditions from normal or other diagnoses.

Keywords optical biopsy; tissue spectroscopy; optical diagnosis of cancer; noninvasive diagnostics.

1 INTRODUCTION

There are several diseases of the gastrointestinal (GI) tract that are correlated with a predisposition for cancer, including active colitis and Barrett's esophagus. Typically these diseases are followed by annual (or more frequent) endoscopic examination accompanied by tissue biopsies. As many as 20 to 30 biopsies may be taken in one session. This is a time-consuming (and therefore expensive) procedure, which entails some degree of risk for the patient. Optical diagnostic techniques offer the potential for improving disease management. An "optical biopsy" technique, such as the one described in this paper, would not require the removal of tissue. Therefore, the health risks to the patient associated with tissue removal would be eliminated. These risks include possible infection and/or perforation of the organ. Moreover, optical diagnostic techniques can be faster than conventional biopsy followed by histology. For each conventional biopsy, the biopsy tool must be withdrawn from the endoscope and the specimen removed before the tool can be reinserted for the next biopsy. In contrast, an optical diagnostic probe could be moved from site to site in succession, with each measurement being recorded in a fraction of a

second, by simply moving the location of the probe tip. The result is a faster procedure with reduced trauma to the patient. Finally, since optical diagnostics have the potential to provide diagnosis in real time, they allow treatment to begin immediately.

A range of spectroscopies have been investigated for optical diagnosis, all of which have one basic principle in common. The specific optical spectrum of a tissue sample contains information about the biochemical composition and/or the structure of the tissue. This basic approach is useful not only for the detection of cancer, but may also be used for other diagnostic applications such as blood oxygen saturation and intraluminal detection of atherosclerosis.

While elastic-scattering, fluorescence, infrared and Raman spectroscopies have all been investigated as methods for distinguishing malignant tissue, the majority of *in vivo* work by various groups has utilized laser-induced fluorescence spectroscopy (LIFS). LIFS has been investigated with and without the aid of exogenous drugs that target malignant tissue. The fluorescence from such drugs provides a large signal, which can be helpful in the detection process¹ and may be used as a detection tool for imaging the patterns of malignancy in a

Address all correspondence to Irving J. Bigio. E-mail: ijb@lanl.gov

given area of tissue. This, however, is not an ideal solution for routine screening, since the administration of an exogenous drug is essentially an invasive process and can result in undesirable side effects. When LIFS (usually with UV excitation) is used to detect intrinsic tissue fluorescence, or autofluorescence, as the diagnostic marker,²⁻⁵ it becomes non-invasive, although concerns may arise when significant fluences of UV illumination are used. Svanberg et al. have developed imaging techniques using LIFS, and have investigated its use in several areas of the body, including the brain, bladder, and oral cavity.^{6,7} The results from the LIFS studies involving larger numbers (say ≥ 50) of measurement sites^{5,8,9} demonstrate levels of reliability that range from very good ($>90\%$ specificity, with minimal false negatives) to what is probably unacceptable ($<80\%$ specificity, with a significant fraction of false negatives). In the case of autofluorescence, changes in the concentration of reduced nicotinamide dinucleotide (NADH) or the redox state of flavin cofactors flavin mononucleotide or flavin adenine dinucleotide are often cited as the presumed origin of the fluorescence spectral signatures¹⁰⁻¹² that correlate with tissue pathologies; however, some authors have noted that it is difficult to separate changes in fluorophore concentration from variations in detected intensities due to scattering effects caused by changes in the epithelial cellular structure.^{5,13}

Although *in vitro* work for detecting malignancy with infrared absorption spectroscopy^{14,15} and Raman spectroscopy^{16,17} has been published, we are not aware of any publications in the open literature dealing with *in vivo* measurements. The potential advantage of either IR or Raman spectroscopy is that the spectral features are relatively sharp, and are specific to the known compounds in the tissue. A technical challenge for noninvasive *in vivo* IR absorption spectroscopy would be the absorption by water itself, which overlaps many of the interesting biomolecular vibrational modes. Raman spectroscopy, on the other hand, can be done with visible or near-IR excitation wavelengths, so that the Raman-shifted scattered light is still at wavelengths where water is essentially transparent. However, the effective signal strength for Raman scattering is much weaker than for LIFS or IR spectroscopy. Recent technological advances, especially in CCD detectors and diode lasers, have reduced the Raman collection time significantly,¹⁸ opening the door to clinical application. The potential for Raman spectroscopy to diagnose breast tissue¹⁶ and gynecological tissues¹⁷ has been investigated *in vitro*. While initial measurements to differentiate malignant and non-malignant tissue with Raman spectroscopy show promise, *in vivo* studies with a significant number of patients will be needed for conclusive results, and the instrumentation remains expensive.

In the work presented here, the signatures for tissue diagnosis are generated by the use of elastic-

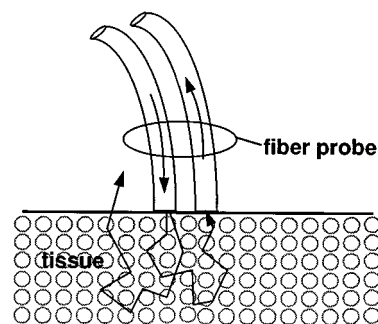


Fig. 1 The optical geometry of the fiber probe, used in optical contact with the tissue surface.

scattering spectroscopy (ESS). Tissue pathologies are detected and diagnosed using spectral measurements of the elastic-scattered light, in a manner that is sensitive to both scattering and absorption properties of the tissue, over a wide range of wavelengths. The use of a technique that is sensitive to the wavelength dependence of scattering efficiency and angles, as well as to absorption bands, is based on the fact that many tissue pathologies, including a majority of cancer forms, exhibit significant architectural changes at the cellular and sub-cellular level. The intent with this approach is to generate spectral signatures of relevance to the tissue parameters that pathologists address. After preparing a slide, a pathologist performs a microscopic assessment (histopathology) of the cell architecture or morphology: the sizes and shapes of cells, the ratio of nuclear to cellular volume, the form of the bilipid membrane, clustering patterns, etc. Since the cellular components that cause elastic scattering have dimensions typically on the order of visible to near-IR wavelengths, the elastic scattering properties will exhibit a wavelength dependence that is more complex than for simple ($1/\lambda^4$) Rayleigh scattering. When source and detector fibers are sufficiently separated for the diffusion approximation to be valid (typically ≥ 0.5 cm), the spectral dependence of the collected light will be insensitive to the size and shapes of the scattering centers. However, for small separations (≤ 0.1 cm), as with our endoscope-compatible probe, the wavelength dependence is readily measured. Thus, for such geometries, morphology and size changes can be expected to cause significant changes in an optical signature that is derived from the wavelength dependence of elastic scattering. These principles underlying ESS have been discussed in earlier publications.^{19,20}

The ESS probe is designed to be used in optical contact with the tissue under examination and has separate illuminating and collecting fibers. Thus, the light that is collected and transmitted to the analyzing spectrometer must first undergo multiple scattering through a small volume of the tissue before entering the collection fiber(s) (see Figure 1).

(No light is collected from surface reflection, specular or diffuse, and we submit that ESS is a more accurate name for our method than "reflectance" spectroscopy.) The resulting effective path length of the collected photons is generally several times greater than the actual separation of the fiber tips. Consequently, the system has good sensitivity to the optical absorption bands of the tissue components, over its effective operating range of 300 to >750 nm, and such absorption features add valuable complexity to the scattering spectral signature. It is important to note that the fiber probe, being used in optical contact with the tissue, examines only that site and does not image the tissue surface.

Although the instrument used in these experiments generates a spectrum that reflects the wavelength dependencies of both scattering and absorption without separating those contributions, these composite signatures appear to correlate well with differences in tissue types and condition. The potential of this technique *in vivo* has recently been demonstrated in the bladder where a sensitivity and specificity of 100 and 97% were obtained in preliminary clinical studies.²¹

Elastic scattering spectroscopy offers some advantages over LIFS. Less expensive detectors can be used because the optical signals are much stronger with ESS. Furthermore, a white-light source can be employed rather than a laser. The data acquisition and storage/display time with our instrument is <1 s. Thus, in addition to the reduced invasiveness of this technique compared with current state-of-the-art methods (surgical biopsy followed by microscopic examination), ESS offers the possibility of impressively faster diagnostic assessment.

2 MATERIALS AND METHODS

The system, depicted schematically in Figure 2, consists of a white light source, fiber optic delivery and collection fibers, spectrometers for dispersion of the collected light and linear CCDs for detection. The wavelength range of the system is 300 to 750 nm. The white light source is a xenon arc lamp (Hamamatsu L2193, Bridgewater, New Jersey) with an elliptical reflector for focusing the light into the illuminating fibers. Two pairs of spectrometer/detectors are employed, with one measuring the signal returned by the collection fiber from the tissue, and the other being used to measure a reference spectrum from a "standard" scattering material (Spectralon, Labsphere, Inc., North Sutton, New Hampshire), which has a very flat diffuse reflectance >98% over the wavelength range of our system. The purpose of the reference standard is to normalize the data against overall system response and changes due to variations in lamp spectral and temporal output, thermal effects on system response, imperfect coupling of the fiber probe, etc.

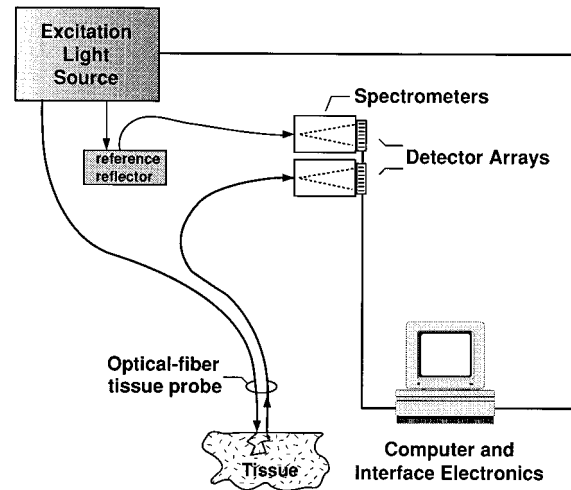


Fig. 2 Schematic diagram of the experimental system. The light source is a xenon short-arc lamp. The dual spectrometers are on computer boards and are actually located inside the computer.

(A reference material with any spectral variations in its diffuse reflectance would result in altered tissue signatures.)

The spectrometers and detectors are integrated on PC-compatible computer boards (Ocean Optics, Dunedin, Florida). High OH⁻ optical fibers, 200 to 500 μm in diameter, were used for light delivery and collection. The complete optical probe, including an outer jacket, is <2 mm in diameter and fits through the working channel of the endoscopes. The small diameter of the probe requires that the source and collection fibers be in close proximity to each other: 300 to 400 μm center-to-center for the data presented in this paper. Thus, only a small volume of tissue, $\leq 1 \text{ mm}^3$, is examined with each measurement. More detailed discussions of the operating principles and specifications of our instrumentation have appeared in earlier publications.^{22,23} It should be noted that the general character of measured spectra would be somewhat sensitive to the fiber size and separation. However, the metrics that are successfully applied to data from both the Medical College of Wisconsin (MCW) and the Baptist Medical Center in Oklahoma City (BMCO) are acceptably robust to these parameters. Nonetheless, a reduced data spread can be achieved with consistent fiber-probe dimensions, and future studies will incorporate standardized probe designs.

3 IN VIVO MEASUREMENTS AND RESULTS

Measurements were made at two clinical sites, the Froedtert Memorial Hospital of the Medical College of Wisconsin in Milwaukee, and BMCO. At each of the clinical sites, histology was performed by only one pathologist. (A more reliable "gold standard" can be achieved with assessment by a panel of pathologists, and the commercial Food and Drug

Table 1 Breakdown of rectal and colon patients and biopsies by pathological diagnoses.

	Total number	Normal	Colitis, Inflammatory bowel disease, Crohn's	Hyperplasia	Adenomas	Adeno-carcinoma
Patients at MCW	5	3	3	0	1	0
Biopsies at MCW	40	13	24	0	3	0
Patients at BMCO	10	7	4	1	3	1
Biopsies at BMCO	20	8	7	1	3	1

Administration (FDA) trials discussed in the conclusions invoke such a panel.) After the first clinical measurements, at MCW, small adjustments in the measurement system were made to improve its performance and reliability. For example, in order to eliminate variability in the transmission efficiency of the probe fibers caused by bending of the guiding endoscope, loops of about 5 cm diameter were made in a segment of the fiber bundle before the endoscope. This blocks transmission of the marginally transmitted high-angle modes in the fibers and eliminates any system sensitivity to flexing of the distal end of the endoscope. While the collection fiber was always 200 μm in diameter, it was also determined that several 200- μm illumination fibers offered the advantage of enhanced flexibility over one 500- μm fiber, an important feature when used with highly flexible colonoscopes.

For the measurements described in this section, all the spectra have been normalized to the same total integrated signal from 350 to 700 nm. Thus all comparisons of spectral features are independent of the overall spectral amplitude.

Data were taken from the lower GI tract and the stomachs of 32 patients. Measurements were made on the lower GI tract (colon, rectum) of 5 patients at MCW and 10 patients at BMCO, and the stomach data were taken with 5 patients at MCW and 12 patients at BMCO. Tables 1 and 2 summarize the patient and pathology classifications. For each optical measurement, the fiber probe was placed in gentle contact with the tissue to be examined, and

the system was then triggered (e.g., with a foot pedal) to make a measurement. The fiber probe was then retracted, and the standard biopsy tool was inserted to take a tissue sample from precisely the same location where the optical measurement was made. Each spectral file was properly identified to correlate to its corresponding tissue sample. In this way we obtained clear one-to-one correspondence between optical measurements and histology reports.

Figure 3 shows an example of spectra taken from the colon of one patient at BMCO. The absorption bands of oxyhemoglobin (the Soret band and Q bands) are clearly evident. Spectra from other patients and/or other parts of the GI tract vary in detail, but are similar in general character. The spectral changes associated with different diagnoses were generally greater than the spectral variations from patient to patient for the same diagnosis (e.g., normal). Spectral changes for different organ and tissue types were also large. In Figure 3 some spectral signature differences are evident by inspection. Based on inspection of the spectra from several patients, we establish a spectral signature "identifier," in this case for changes in colon diagnosis, to separate dysplastic (generally assumed as having the potential to become malignant) and malignant conditions from more benign conditions, such as hyperplasia, inflammation and colitis, as well as normal mucosa.

Table 2 Breakdown of stomach patients and biopsies by pathological diagnoses.

	Total number	Normal	Inflamed/gastritis	Hyperplastic	Atypia/dysplasia
Patients at MCW	5	4	1	0	0
Biopsies at MCW	15	11	4	0	0
Patients at BMCO	12	4	8	1	1
Biopsies at BMCO	22	9	11	1	1

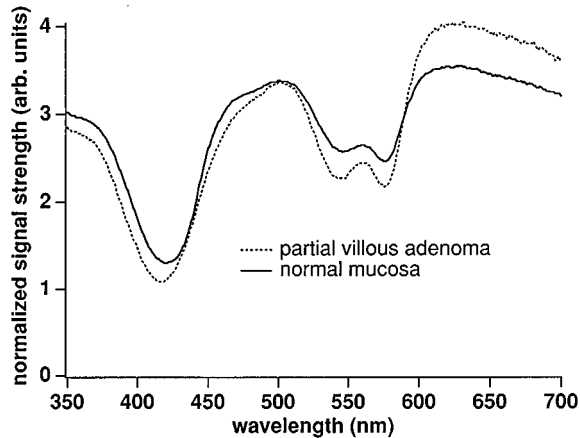


Fig. 3 Typical tissue spectra, shown as examples, for two measurements made in the colon of one patient. The spectra have been normalized to the same total integrated signal between 350 and 700 nm.

3.1 COLON/RECTUM: IDENTIFICATION OF DYSPLASIA AND CARCINOMA

Figure 4 shows the data from measurements in all patients (15) with colon and rectal abnormalities, from both MCW and BMCO. Since most of the rectum, until the last few centimeters, has the same type of epithelium as the colon, it is reasonable to display the data from both on the same spectral graph. (All of our rectal data were taken at sites more than 5 cm from the anus.) For each of the 60 biopsy sites, the integrated spectral values for two segments of the spectrum are plotted against each other. That is, for each measurement site, the spectrum integral from 540 to 580 nm is plotted against the integral from 400 to 440 nm, in a two-variable

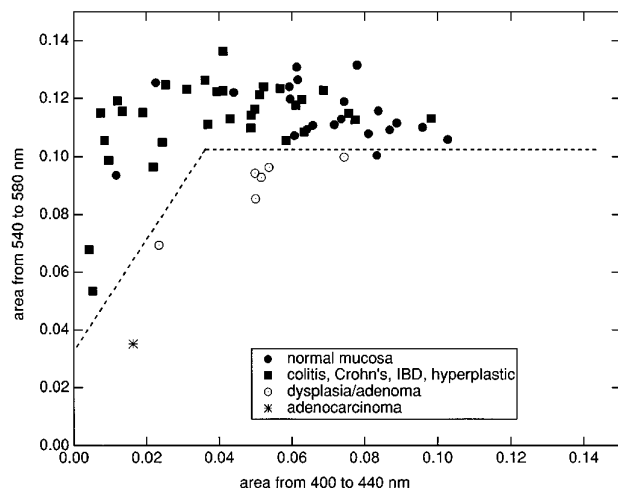


Fig. 4 Data from the colons and rectums of 15 patients at both clinical sites are plotted against two spectral markers as noted on the graph. The dashed lines separating the diagnostic zones have been drawn to minimize false negatives at the expense of enclosing one or two false positives.

graph. The pathologists' diagnoses from the corresponding actual biopsies are designated by the data-point symbol.

The 400 to 440-nm segment clearly encloses the hemoglobin (Hb) Soret band, but also encompasses some absorption from compounds such as flavin mononucleotide, beta carotene, bilirubin, cytochrome, etc.; whereas the 540 to 580-nm segment covers the Hb Q band, with minor absorption from cytochrome and other components. As has been the case with most work published on spectroscopic diagnostics, we can only speculate about the underlying changes responsible for the spectral-diagnostic differences in our data. The data in Figure 4 appear generally to reflect relative changes in the Soret-band absorption versus the Q-band absorption. Several different explanations for this are consistent with the data. The spectral changes can be caused by changes in the oxygen saturation of the Hb. However, since the optical geometry of our fiber probe, and the physics of elastic scattering, are such that collected photons at longer wavelengths, on average, will have probed a somewhat deeper sampling of tissue than the shorter wavelengths, it is also plausible that the spectral changes reflect differences in the depth and extent of microvascular perfusion. Moreover, it is equally likely that the spectral changes are due to alterations in the wavelength dependence of the elastic scattering caused by changes in the average size, shape, or refractive index of the scattering centers. A separate, large-scale, rigorous study of *in vitro* samples—such a study would not be practical under *in vivo* conditions—would be required to establish the relative importance of the various factors contributing to the spectral changes.

The area below the dashed lines in Figure 4 represents our arbitrarily chosen diagnostic criteria for carcinomas and adenomas, the types of diagnoses of greatest concern to physician and patient. The locations of the lines have been chosen to obviate false negatives at the expense of enclosing a small percentage of false positives. Although the desired separation in this graph appears good, one must note that the paucity of malignant and dysplastic diagnoses limits the conclusions. Nonetheless, the results are promising enough to warrant further study and more statistics.

It is also possible that a different spectral feature would yield a more impressive separation of dysplastic conditions from other, more benign, diagnoses. The issue of finding the best spectral signatures is discussed near the end of this paper.

3.2 COLON: SEPARATION OF COLITIS FROM NORMAL MUCOSA

Although the spectral signature used for Figure 4 differentiates dysplastic and malignant diagnoses from other indications, the separation of nondysplastic colitis from normal colorectal mucosa is less

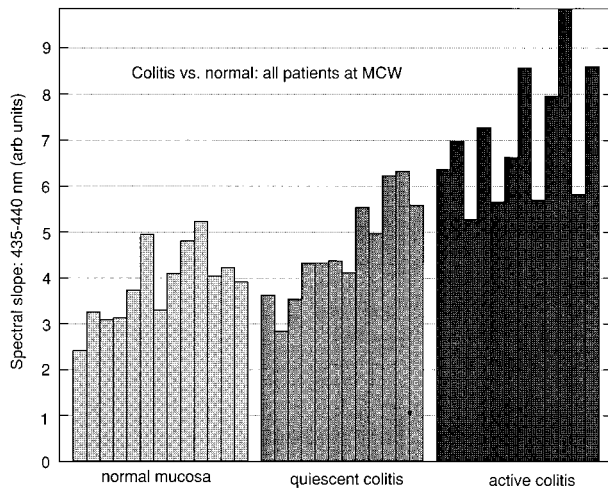


Fig. 5 One spectral signature that shows significant separation of chronic active colitis from quiescent colitis and normal mucosa, applied to patients from MCW.

successful. Therefore we tested other spectral signatures in an attempt to show a better spectral differentiation between colitis and normal colon mucosa. As an example, Figure 5 shows data from the 5 lower-GI patients at MCW, for which a simple spectral signature (different from that used to distinguish dysplasia) reasonably separates active colitis from quiescent colitis and normal colon mucosa. The signature used is the slope of the spectrum in the 435 to 440-nm range.

3.3 STOMACH: IDENTIFICATION OF ABNORMALITIES

Data were also taken and correlated with biopsy reports for 37 measurement sites in 17 patients with gastric problems. Only one corresponding pathology report indicated dysplasia, and none were malignant. The results of one possible spectral analysis are displayed in Figure 6. The first 11 data bars for

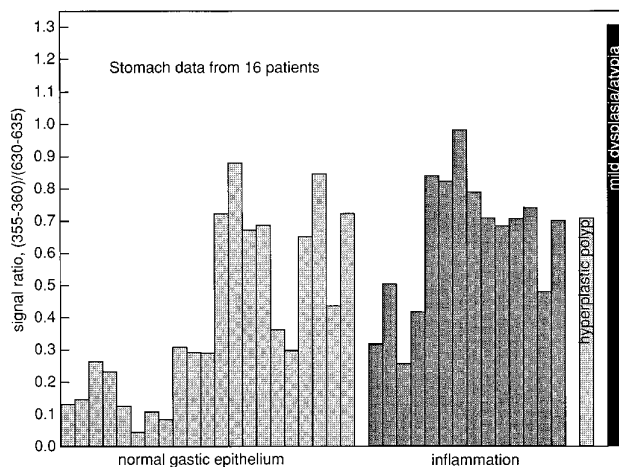


Fig. 6 Data from 37 pathology reports on stomach (gastric) epithelium for 17 patients.

normal mucosa and the first 4 data bars for inflammation are from patients at MCW, while all the remaining bars are from BMCO. The spectral data as displayed show an easy separation of the one dysplastic biopsy from all the others, using as the optical signature the ratio of signal strengths in the near UV (355 to 360 nm) to that in the red (630 to 635 nm). (As can be seen, the spectral signature values for measurements at MCW are generally lower than the corresponding values from BMCO. This is attributable to a difference in the optical system calibrations at the two hospitals, which caused a difference in the signal levels for the UV wavelengths only.) The increase in the plotted spectral scattering ratio for the dysplastic biopsy site would be consistent with a decrease in the average size of the scattering centers, as might occur with an infiltration of lymphocytes. However, with only one dysplastic data point, no conclusions can be drawn about the selected spectral signature, and further studies will be required to provide data from a larger number of dysplastic sites. Thus, Figure 6 is provided for information purposes only.

4 DISCUSSION AND FUTURE DIRECTIONS

We wish to emphasize that in all the measurements presented here we did *not* individually normalize any spectrum against that from a nearby putative normal tissue site for the same patient. This is because we wished to determine whether any spectral signatures found in the analyses were robust with respect to patient-to-patient variations. Generally, this is similar to the conditions under which a pathologist makes a diagnosis: the biopsy sample is identified by the organ it came from, but a nearby "normal" biopsy sample is typically not supplied. Nonetheless, in future studies, increased reliability may be achieved by local normalization within the same patient.

In addition to storing the data, our system displays the acquired spectrum immediately (in less than 1 s). Ultimately, we would expect the physician to be able to determine the diagnosis immediately by looking at the data on the screen, probably assisted by a display of the computer's analysis of the spectrum. However, for these preliminary studies, our general procedure was to store the data and later compare spectra with the coordinated pathology reports. By simple visual examination of the data from a subset of the patients, we were often able to identify one or more spectral variations corresponding to different pathology reports. We would then apply that signature to the entire patient data set and assess the degree of reliability of the correlation with pathology. Thus, in all the data analyses presented above, the selective spectral signatures were determined "by inspection" together with some trial and error.

The use of simple visual examination of the spectra in determining patterns and signature differ-

ences, which has been employed for fluorescence spectral analysis by several other groups (e.g., see Refs. 2, 8, 24), is not as simplistic a method as one might think. The power of the eye/brain to recognize patterns (of two-dimensional spatial information, such as an image) under a variety of circumstances can exceed the capabilities of the most powerful computers. In the case of "one-dimensional" spectral information, this power is invoked by displaying information as a two-dimensional plot: i.e., a spectrum of signal versus wavelength. However, often several possible options appear upon first observation, and it is generally difficult to determine which among them will yield the largest and most reliable differentiation. This results in numerous iterations of data analysis. Succinctly, since well-understood algorithms have been developed for **one-dimensional** data analysis, computers can be very effective, especially when the spectrum is composed of multivariate components. Therefore, it would be very helpful to be able to employ mathematical methods to rapidly identify the most reliable spectral signature differences, and to determine which option among several is likely to be the most reliable. Consequently, in addition to improvements in the stability of the spectral response of the system, our future plans include computational automation for identification of the spectral signatures, for each pathology and tissue type, that will provide the most reliable diagnostic differentiation.

The key to analyzing tissue spectral data lies not only in choosing an appropriate data analysis technique, such as principal component analysis or neural networks, but in pretreating the data to enhance features so that accurate predictions can be made. Among the steps toward developing computational algorithms for rapidly identifying spectral signatures for tissue conditions is the development of an extensible preprocessor for the data to select features in the data as candidates for predictors. Analysis techniques, such as multivariate linear regression analysis, have been used with some success in analyzing fluorescence data where assumptions can be made about the likely major contributors,^{5,9,25,26} and the partial least-squares method has been applied to specific infrared spectra for glucose monitoring.²⁷ These may be helpful, assuming knowledge of the sources of some of the absorption bands. However, given the complexity of interrelating spectral effects of scattering and absorption, methods that require no *a priori* knowledge of constituents, such as neural net methods and soft independent modeling of class analogy (SIMCA)²⁸ may be more practical.

5 CONCLUSIONS

We have conducted preliminary clinical testing of elastic-scattering spectroscopy as a method for diagnosing pathologies of the gastrointestinal tract.

Data from the colon, rectum, and stomach appear promising for detecting dysplasia. Improved detector stability, better standardization of probes and calibration, assessment by a pathology panel, and more sophisticated spectral data analysis may improve the reliability of correlating spectral data with pathology reports. At the time of this writing, FONET, Inc., which has licensed this technology from University of California/Los Alamos National Laboratory, has begun FDA-approved trials at a number of medical centers. These trials are determining the efficacy of the technology for diagnosis of malignant and dysplastic conditions in the bladder and colon. While the data presented in this paper indicate proof of concept and are promising, the results from the FDA trials should provide a much larger statistical database for rigorous evaluation of elastic-scattering spectroscopy as a method for non-invasive diagnostics.

Acknowledgments

The authors appreciate the assistance with the data analysis ably provided by Kira Rand Giovanielli.

REFERENCES

1. D. Kessel, "Tumor localization and photosensitization by derivatives of hematoporphyrin: A review," *IEEE J. Quantum Electron.* **23**, 1718-1720 (1987).
2. R. R. Alfano, D. B. Tata, J. Cordero, P. Tomashefsky, F. W. Longo, and M. A. Alfano, "Laser induced fluorescence spectroscopy from native cancerous and normal tissue," *IEEE J. Quantum Electron.* **20**, 1507-1511 (1984).
3. R. M. Cothren, R. Richards-Kortum, M. V. Sivak, M. Fitzmaurice, R. P. Rava, G. A. Boyce, M. Doxtader, R. Blackman, T. B. Ivanc, G. B. Hayes, M. S. Feld, and R. E. Petras, "Gastrointestinal tissue diagnosis by laser induced fluorescence spectroscopy at endoscopy," *Gastrointest. Endosc.* **36**, 105-111 (1990).
4. R. Richards-Kortum, R.P. Rava, R.E. Petras, M. Fitzmaurice, M. Sivak, and M.S. Feld, "Spectroscopic diagnosis of colonic dysplasia," *Photochem. Photobiol.* **53** (6), 777-786 (1991).
5. K. T. Schomacker, J. K. Frisoli, C. C. Compton, T. J. Flotte, J. M. Richter, N. S. Nishioka, and T. F. Deutsch, "Ultraviolet laser-induced fluorescence of colonic tissue: basic biology and diagnostic potential," *Lasers Surg. Med.* **12**, 63-78 (1992).
6. K. Svanberg, S. Andersson-Engels, L. Baert, E. Bak-Jensen, R. Berg, A. Brun, S. Colleen, I. Idvall, M. D'Hallewin, C. Ingrar, J. Johansson, S. Karlsson, R. Lundgren, L.G. Salford, U. Stenram, L. Strömbald, S. Svanberg, and I. Wang, "Tissue characterization in some clinical specialties utilizing laser-induced fluorescence," *Proc. SPIE* **2135**, 2-15 (1994).
7. S. Andersson-Engels, J. Johansson, K. Svanberg, and S. Svanberg, "Laser-induced fluorescence in medical diagnostics," *Proc. SPIE* **1203**, 76-96 (1990).
8. T. Vo-Dinh, M. Panjehpour, B. F. Overholt, C. Farris, F. P. Buckley III, and R. Sneed, "In vivo cancer diagnosis of the esophagus using differential normalized fluorescence (DNF) indices," *Lasers Surg. Med.* **16**, 41-47 (1995).
9. N. Ramanujan, M. F. Mitchell, S. Warren, S. Thomsen, E. Silva, and R. Richards-Kortum, "In vivo diagnosis of cervical intraepithelial neoplasia using 337-nm-excited laser-induced fluorescence," *Proc. Natl. Acad. Sci. U.S.A.* **91**(21), 10193-10197 (1994).
10. W. Lohman et al., "Native fluorescence of the cervix uteri as a marker for dysplasia and invasive carcinoma," *J. Obstet. Gynecol. Reprod. Biol.* **31**, 249-253 (1989).
11. S. Andersson-Engels, J. Johansson, K. Svanberg, and S. Svanberg, "Fluorescence imaging and point measurements of tissue: applications to the demarcation of malignant tu-

- mors and atherosclerotic lesions from normal tissue," *Photochem. Photobiol.* **53**, 807-814 (1991).
12. J. Beuthan, Ch. Zur, F. Fink, and G. Müller, "Laser fluorescence spectroscopic experiments for metabolism monitoring," *Lasers Med. Surg.* **6**, 72-75 (1990).
 13. G. Bottioli, A.C. Croce, D. Locatelli, R. Marchesini, E. Pignoli, S. Tomatis, C. Cuzzoni, S. Dipalma, M. Dalfante, and P. Spinelli, "Natural fluorescence of normal and neoplastic human colon: a comprehensive ex vivo study," *Lasers Surg. Med.* **16**, 48-60 (1995).
 14. P. T. T. Wong, R.K. Wong, and M.F.K. Fung, "Pressure-tuning FT-IR study of human cervical tissues," *Appl. Spectroscopy* **47**, 1058-1063 (1993).
 15. P. T. T. Wong, S. Lacelle, and H. M. Yazdi, "Normal and malignant human colon tissues investigated by pressure-tuning FT-IR spectroscopy," *Appl. Spectroscopy* **47**, 1830-1836 (1993).
 16. D. C. B. Redd, Z. C. Feng, K. T. Yue, and T. S. Gansler, "Raman spectroscopic characterization of human breast tissues: implications for breast cancer diagnosis," *Appl. Spectroscopy* **47** (6), 787-791 (1993).
 17. C. H. Liu, B. B. Das, W. L. Sha Glassman, G. C. Tang, K. M. Yoo, H. R. Zhu, D. L. Akins, S. S. Lubicz, J. Cleary, R. Prudente, E. Celmer, A. Caron, and R. R. Alfano, "Raman, fluorescence, and time-resolved light scattering as optical diagnostic techniques to separate diseased and normal biomedical media," *J. Photochem. Photobiol. B: Biol.* **16**, 187-209 (1992).
 18. J. J. Baraga, M. S. Feld, and R. P. Rava, "Rapid near-infrared Raman spectroscopy of human tissue with a spectrograph and CCD detector," *Appl. Spectroscopy* **46** (2), 187-190 (1992).
 19. James Boyer, Judith R. Mourant, and Irving J. Bigio, "Theoretical and experimental investigations of elastic scattering spectroscopy as a potential diagnostic for tissue pathologies," in *Proc. OSA: Advances in Optical Imaging and Photon Migration*, R. R. Alfano, ed., Vol. 21, pp. 265-268, Optical Society of America, Washington, DC (1994).
 20. James Boyer, Judith R. Mourant, and Irving J. Bigio, "Monte Carlo investigations of elastic scattering spectroscopy applied to latex spheres used as tissue phantoms," *Proc. SPIE* **2389**, 103-112 (1995).
 21. Judith R. Mourant, Irving J. Bigio, James Boyer, Richard I. Conn, Tamara Johnson, and Tsutomu Shimada, "Spectroscopic diagnosis of bladder cancer with elastic light scattering," *Lasers Med. Surg.* **17**, 350-357 (1995).
 22. Irving J. Bigio, Thomas R. Loree, Judith Mourant, Tsutomu Shimada, K. Story-Held, R. D. Glickman, and Richard Conn, "Optical diagnostics based on elastic scattering: recent clinical demonstrations with the Los Alamos Optical Biopsy System," *Proc. SPIE* **2081**, 174-184 (1993).
 23. Irving J. Bigio, Judith R. Mourant, James Boyer, Tamara Johnson, and Tsutomu Shimada, "Noninvasive identification of bladder cancer with sub-surface backscattered light," *Proc. SPIE* **2135**, 26-31 (1994).
 24. Y. Yang, G. C. Tang, M. Bessler, and R. R. Alfano, "Fluorescence spectroscopy as a photonic pathology method for detecting colon cancer," *Lasers Life Sci.* **6**, 259-276 (1995).
 25. E. J. Gaffney, R.H. Clarke, A.R. Lucas, and J.M. Isner, "Correlation of fluorescence emission with plaque content and intimal thickness of atherosclerotic coronary arteries," *Lasers Med. Surg.* **9**, 215-228 (1989).
 26. L. I. Deckelbaum, M.L. Stetz, K.M. O'Brien, F.W. Cuttrazzola, A.F. Gmitro, L.I. Laifer, and G.R. Gindi, "Fluorescence spectroscopy guidance of laser ablation of atherosclerotic plaque," *Lasers Med. Surg.* **9**, 205-214 (1989).
 27. D. M. Haaland, M. R. Robinson, G. W. Koepp, E. V. Thomas, and R. P. Eaton, "Reagentless near-infrared determination of glucose in whole blood using multivariate calibration," *Appl. Spectroscopy* **46**, 1575-1578 (1992).
 28. S. Wold and M. Sjostrom, "SIMCA: a method for analyzing chemical data in terms of similarity and analogy," in *Proc. Chemometrics: Theory and Application*, ACS Series, Vol. 52, pp. 243-282 (1977).